HAMAMATSU
PHOTON IS OUR BUSINESS

Measuring the electrical and optical properties of the MPPC silicon photomultiplier

By Slawomir Piatek, Hamamatsu Corporation & New Jersey Institute of Technology (February 2014)

Understanding the operation of a Multi-Pixel Photon Counter (a type of silicon photomultiplier) together with its electrical, optical, and noise characteristics is crucial for the proper interpretation of scientific data obtained with this detector. This article is a literature review of the methods employed in characterizing MPPCs.

Editor's note: Silicon photomultipliers (as they are commonly known) are manufactured by Hamamatsu under the brand name of **Multi-Pixel Photon Counter**.

Introduction

The Multi-Pixel Photon Counter (also known as a silicon photomultiplier or SiPM) is a two-prong photodetector consisting of pixels connected in parallel; one pixel is a series combination of an avalanche photodiode (APD) and a quenching resistor, R_Q (see Figure 1).

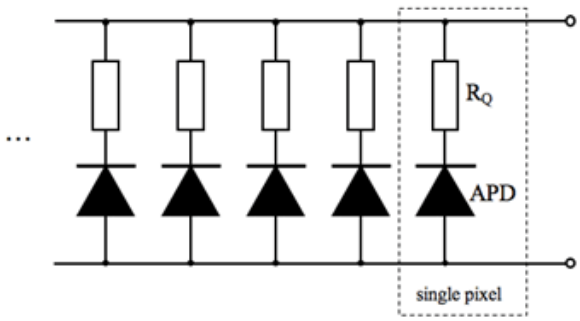

Figure 1. Equivalent circuit of an MPPC. A single pixel is a series combination of an avalanche photodiode and a quenching resistor. All of the pixels are connected in parallel.

In a typical operation, an MPPC is externally reverse-biased with a V_{BIAS} that is up to a few volts greater than the breakdown voltage (V_{BR}) of the APD. An overvoltage, $\Delta V \equiv V_{BIAS} - V_{BR}$, is one of the most important adjustable parameters affecting the performance of the detector, controlling its optical and electrical characteristics such as the gain (M), photon detection efficiency (PDE), and the rates of dark counts, afterpulsing, and optical crosstalk.

In the absence of light and ignoring dark counts, there is no current flowing through a pixel; thus, the voltage on the APD equals V_{BIAS}. That APD is said to be in Geiger mode – a highly unstable state that can be disturbed even by a single photon, leading to the formation of a self-sustained avalanche. The role of R_Q in a pixel is to extinguish or quench the avalanche restoring the APD back to Geiger mode. The gain is proportional to the charge released in the avalanche, and its typical values are 10^5 to 10^6. Such a high gain is comparable to that of a photomultiplier tube (PMT), making an MPPC its possible substitute in applications

involving detection of very faint light. The advantages of an MPPC compared to a PMT are a smaller size, immunity to magnetic fields, and lower biasing voltage. The detector's disadvantages are that its performance is sensitive to fluctuations of the ambient temperature and of the biasing voltage, the presence of high rates of thermal noise (~ 1 MHz), and of correlated noise: afterpulsing and crosstalk.

Using an MPPC as a light detector in scientific and clinical research requires that the user of the detector understands its optical and electrical behavior under varied environmental conditions, the types and rates of noise, and the limits on reliable light detection. Although manufacturers of MPPCs provide information on their products, an independent check of the detector characteristics, especially in critical situations where a scientific breakthrough hinges on the validity of the observations, is necessary.

This article is a literature survey of experimental techniques used to characterize optical and electrical properties of an MPPC. Section I describes the basic principles behind the operation of first an APD and then an MPPC. Section II presents and discusses experimental setups to measure the most relevant optical and electrical properties of an MPPC. Section III summarizes the main points of the article.

Section I: Background

A light-sensitive APD is a PN junction normally operated in reverse bias close to its V_{BR}. Unlike a photodiode that has a gain M = 1, an APD can have M > 1 owing to multiplication of the photo-generated charge carrier in the avalanche section of the depletion region by impact ionization. The values of M depend on V_{BIAS} with respect to V_{BR}. The following two subsections describe in greater detail the operation of an APD when $V_{BIAS} < V_{BR}$ and $V_{BIAS} > V_{BR}$, respectively, and an MPPC.

Avalanche photodiode ($V_{BIAS} < V_{BR}$)

A single pixel in an MPPC is an APD connected in series with a resistor. Figure 2 shows a simplified equivalent circuit of an APD operating at reverse bias that is less than V_{BR}. From left to right, the components are current source, ideal diode, junction capacitance (C_J), junction resistance (R_J), and series resistance (R_S).

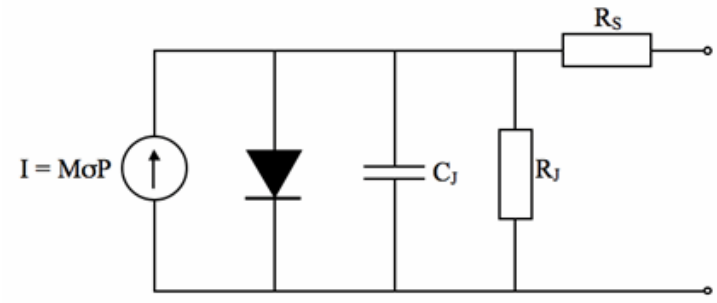

Figure 2. Equivalent circuit of an APD that does not operate in Geiger mode.

The current source outputs current $I = MI_{PH} = M\sigma P$, where M is the gain and I_{PH} is the photocurrent. The gain is a function of applied voltage, whereas $I_{PH} = \sigma P$, where $\sigma=\sigma(\lambda)$ is the spectral photosensitivity and P is the power of the incident light. The gain mechanism is avalanche multiplication of charge carriers by impact ionization in the high field region of the APD. If $V_{BIAS} < V_{BR}$, the avalanche, once triggered, abates completely in finite time.

The behavior of an ideal diode is described by the Shockley equation $I_D = I_0[\exp(V_D/V_T) - 1]$. In this equation, I_D is the current through the diode, I_0 is the reverse saturation current, V_D is the voltage on the diode, and $V_T \equiv kT/e$ is the thermal voltage, where, k is the Boltzmann constant ($k = 8.6 \times 10^{-5}$ eV/K), T is temperature, and e is the magnitude of the charge of the electron ($e = 1.6\times10^{-19}$ C). In a typical operation of an APD, V_D has a large negative value and, thus, $I_D \approx - I_0$ (the minus sign indicates that this is a reverse current). Note that V_D is not an external bias voltage; it is the voltage across the diode and, also, across the current source I, C_J, and R_J.

The capacitor C_J represents the capacitance of the depletion region of the APD. Because the width of the region depends on the voltage across it (which equals V_D), $C_J = C_J(V_D)$. C_J affects the performance of an MPPC in an important way: it controls the shape of the output current pulse. Therefore, measuring its value as a function of V_{BIAS} constitutes a crucial electrical characterization of the device.

The resistor R_J has a value equal to the resistance of the depletion region. The value depends on the width of the region and on the concentration of charge carriers there. R_J is a complicated function of V_D because the latter controls both the width and the degree of impact ionization in the region. When the APD is in Geiger mode and develops an avalanche, R_J becomes negligible.

The resistance R_S equals the combined resistance of the undepleted regions in the APD. The value of R_S depends on V_D since the latter controls the total length of the undepleted regions. R_S is on the order of several hundred ohms at zero bias and decreases to tens of ohms around V_{BR}.

Avalanche photodiode ($V_{BIAS} > V_{BR}$)

When a V_{BIAS} applied to an APD exceeds its V_{BR}, the APD is said to be in Geiger mode. McIntyre (1961) and later Haitz (1964) developed an electrical model (see Figure 3) for an APD operating in this state. Geiger-mode APD is represented by C_J, the switch S, voltage source V_{BR}, and series resistance R_S. In the absence of light and ignoring dark events, the switch S is open and C_J is charged to V_{BIAS}. The voltage on the APD is $\Delta V = V_{BIAS} - V_{BR}$ above V_{BR}, and the APD is in a highly unstable state. Suppose that the APD absorbs a photon and the resulting charge carrier, either an electron or a hole, triggers an avalanche. At this instant, the switch S closes and C_J begins to discharge through R_S, which tends to lower the voltage across the APD. However, since the APD is biased by a constant voltage source V_{BIAS}, current begins to flow through the terminals of the APD reaching a steady state value of $\Delta V/R_S$. This current will persist unless V_{BIAS} is reduced to, or below, V_{BR}; doing so restores the APD to the light-sensitive state.

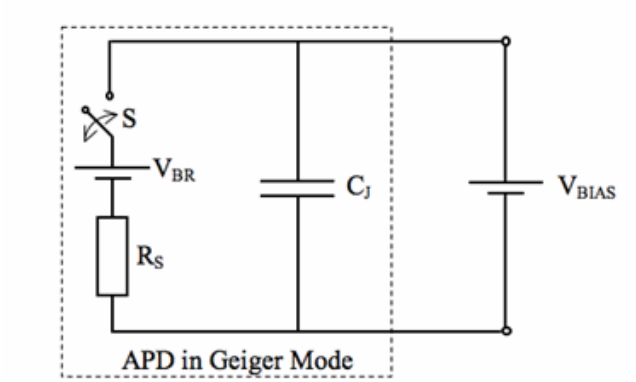

Figure 3. Equivalent circuit of an APD operating in Geiger mode.

Suppose that a resistor $R_Q >> R_S$ is now connected in series with the Geiger-mode APD, as shown in Figure 4.

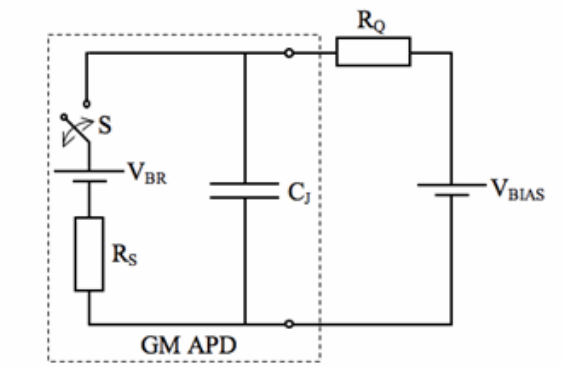

Figure 4. Geiger-mode APD in series with resistor R_Q.

In the absence of light and ignoring dark events, the switch S is open and C_J is charged to V_{BIAS} – no current flows through the APD. The APD is in a photosensitive "ready" state. The switch S closes the instant a photo-generated charge carrier triggers an avalanche. C_J begins to discharge through R_S; this process tends to lower the voltage across the APD and causes a voltage drop across R_Q. The latter implies that a current flows through the terminals of the APD, and Figure 5 depicts its time dependence.

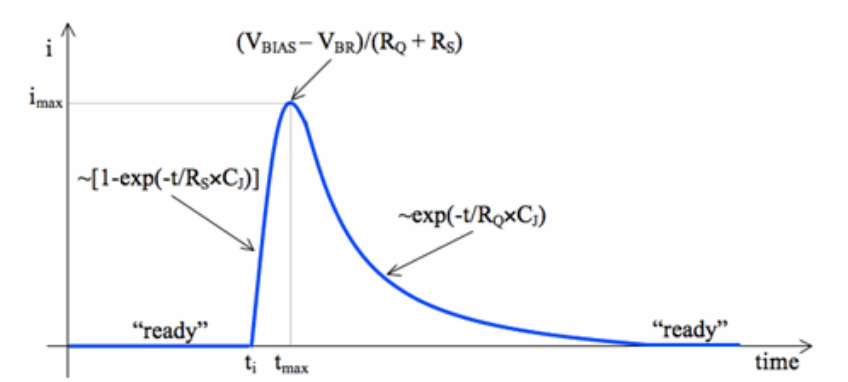

Figure 5. Current flowing through the terminals of the APD as a function of time.

The avalanche begins at $t = t_i$. The leading edge of the current pulse increases with time constant R_SC_J and reaches a maximum value of $i_{max} = (V_{BIAS} - V_{BR})/(R_Q + R_S) \approx \Delta V/R_Q$ at t_{max}. At around this time the avalanche stops or is quenched because of R_Q. After t_{max}, C_J recharges to the nominal voltage of V_{BIAS} while the current decreases with a time constant R_QC_J. Because $R_Q >> R_S$, the leading edge of the pulse is steeper than the trailing (or declining) edge; the pulse is asymmetric around $t = t_{max}$. For a more detailed discussion of the electrical behavior of Geiger-mode APD see Haitz (1964).

MPPCs are designed so that i_{max} (referred to as the "latch" current) is about 20 µA. The condition for proper quenching is $0 < \Delta V < R_Qi_{max}$. For $\Delta V = 1$ V, the minimum R_Q is 50 kΩ. If R_Q is set below this limit, the quenching time increases, which would show as flattening of the current pulse around t_{max}. If R_Q is substantially below the minimum limit, the quenching never occurs and the current becomes constant with an amplitude of $(V_{BIAS} - V_{BR})/(R_Q + R_S)$.

Integrating the current pulse with respect to time yields the total charge Q that transferred between the terminals of the APD. Since the transfer was triggered by a single charge carrier, the gain M = Q/e. A detailed analysis shows that $Q = C_J \Delta V$ and, thus, $M = C_J \Delta V/e$.

MPPC

The MPPC is a rectangular array of light-sensitive elements – pixels – that are all connected in parallel and externally biased by a single voltage source, V_{BIAS}. Each pixel is a series combination of an APD and a resistor R_Q. By design, all pixels are identical. The pixels operate in Geiger mode, that is, $V_{BIAS} > V_{BR}$, or $\Delta V > 0$.

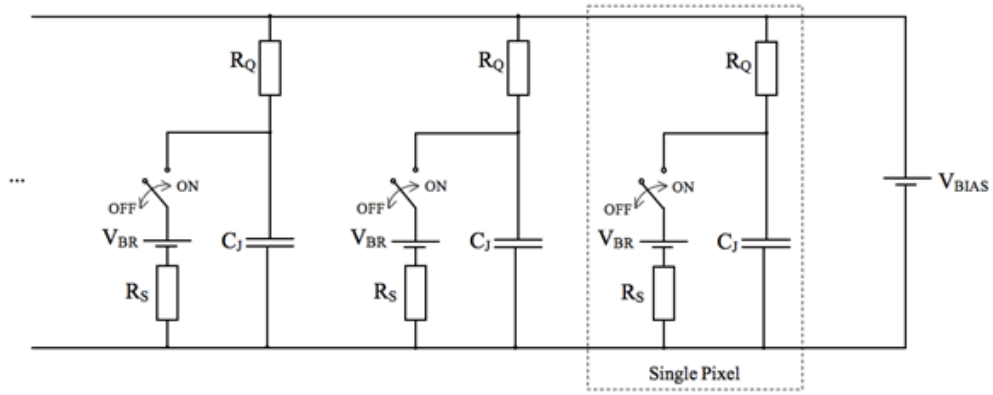

Figure 6. Equivalent circuit of an MPPC.

Figure 6 shows n equivalent circuit of an MPPC; the dotted rectangle delineates a single pixel. In the absence of light and ignoring dark counts, all of the switches are in the OFF position, and the voltage is V_{BIAS} on each APD and is zero on each R_Q. Suppose that a single APD absorbs a photon and the process triggers an avalanche. At this instant, the switch in the equivalent circuit of that APD goes to the ON position, and the current pulse begins to flow through the terminals of the MPPC as shown in Figure 5. R_Q of that pixel quenches the avalanche, and the pixel is restored back to the "ready" state. If two (or more) photons simultaneously trigger avalanches in two (or more) distinct pixels, the current pulse flowing through the terminals of the MPPC is a superposition of the current pulses generated by the two (or more) pixels. In contrast, if a single pixel absorbs simultaneously two or more photons, the ensuing current pulse is identical to the one produced by a single photon.

When a pixel recovers from the avalanche, its C_J recharges to the nominal voltage V_{BIAS}. At the outset of the recharge process, the current flows from V_{BIAS} but also from the junction capacitors of all other pixels. The latter current keeps lowering ΔV on the other pixels until the value equals to the ΔV on the recovering pixel. At this instant, V_{BIAS} becomes the only source of current, and all of the pixels recharge together back to V_{BIAS}.

Section II: Characterization of an MPPC

This section describes experimental methods of measuring electrical and optical characteristics of an MPPC.

Measuring R_Q and C_J

The forward-bias I-V characteristic of an MPPC (e.g., see Figure 10) can be used to measure the approximate value of R_Q. The I-V characteristic can be obtained with a circuit shown in Figure 7. Assuming that R_Q is the

same for each pixel and that $R_Q >> R_S$, the slope of the linear region in the first quadrant equals N/R_Q, where N is the number of pixels. Thus, R_Q = N/slope.

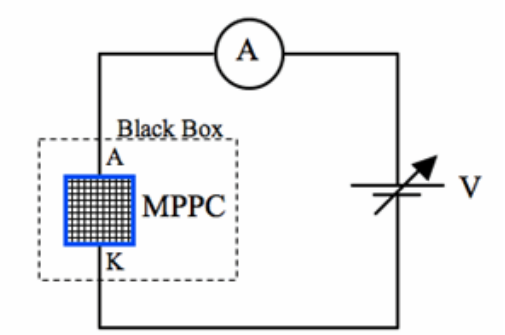

Figure 7. The electrical circuit to obtain a forward-bias I-V characteristic, which contains information about R_Q. The MPPC must be shielded from light in a temperature-controlled environment.

Figure 8 shows an equivalent circuit of an MPPC that illustrates how C_J of a single pixel can be measured. There are N pixels connected in parallel, where one pixel is represented by C_J in parallel with R_J and this combination is in series with $R_S + R_Q$. The terminals of the MPPC are at the right.

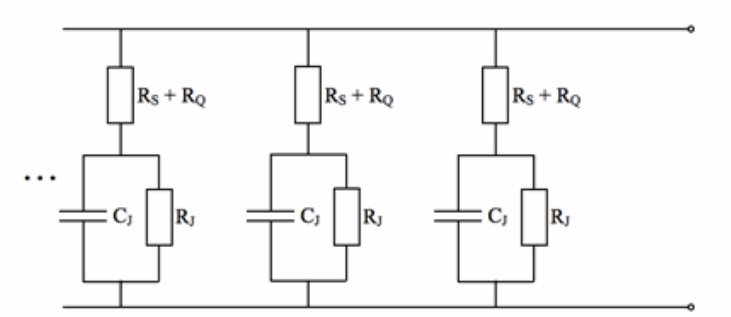

Figure 8. Equivalent circuit of an MPPC to illustrate how to measure C_J.

The impedance Z of the network as seen from the terminals of the MPPC is given by the following equation.

$$Z = \frac{1}{N}\left(R_Q + R_S + \frac{\frac{R_J}{j\omega C_J}}{R_J + \frac{1}{j\omega C_J}}\right) = \frac{R_Q + R_S}{N} + \frac{1}{\frac{N}{R_J} + j\omega N C_J}$$

Equation 1. Impedance of the MPPC shown in Figure 8.

Equation 1 implies that the effective capacitance seen at the terminals of the MPPC is NC_J, the capacitance of a single pixel multiplied by the number of pixels. Because C_J is a function of reverse voltage, the Keithley C-V 590 analyzer is well suited for determining this dependence. Figure 9 shows the block diagram of the experimental setup.

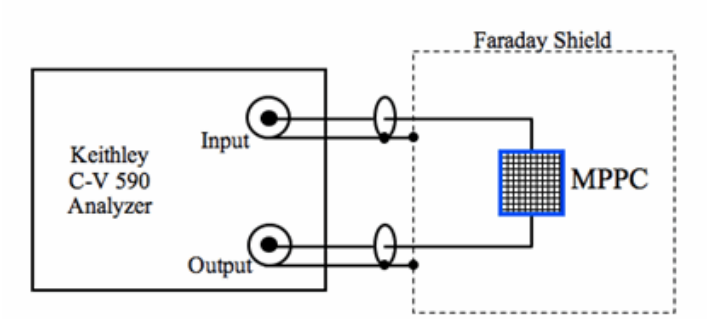

Figure 9. Connection schematic to measure junction capacitance of an MPPC as a function of reverse voltage.

The MPPC is inside a temperature-controlled lightproof Faraday shield. The terminals of the detector are connected to the input and output of the C-V 590 using BNC cables. The "ground" of the cables is connected to the shield. The polarity of the connection is such that when the C-V 590 performs the voltage sweep, the MPPC is reverse-biased.

Figure 10 is an example of forward and reverse I-V and C-V characteristics for an MPPC with 667 pixels. The forward I-V characteristic becomes linear at a bias voltage of around 0.7 V. The inverse of the slope in the linear region is about 225 Ω implying that $R_Q \approx 150$ kΩ. The reverse-bias I-V characteristic shows that the breakdown voltage $V_{BR} \approx 70$ V (reverse).

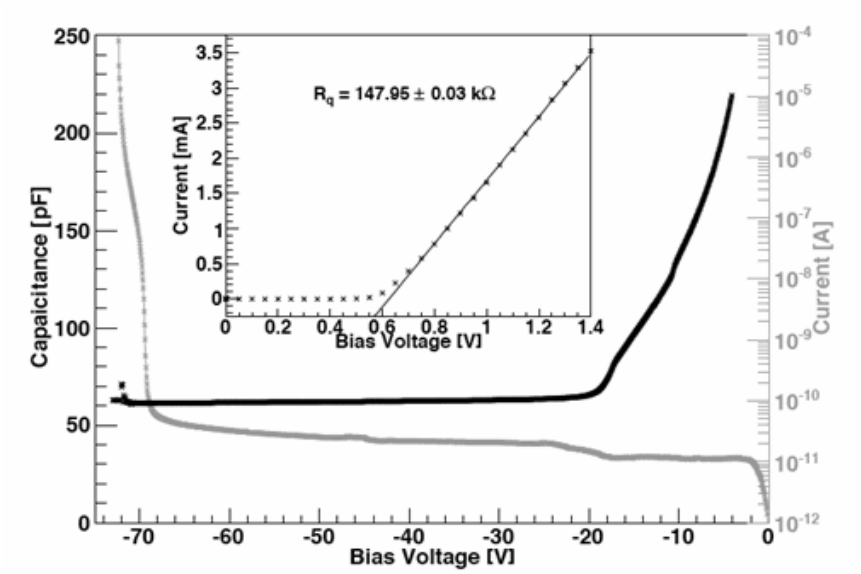

Figure 10. Forward and reverse I-V characteristics and C-V characteristic of an MPPC. Adapted from Vacheret et al. (2011).

The combined junction capacitance N x C_J decreases steeply when the reverse voltage increases from 5 V to 20 V. Above 20 V, the decrease is much less pronounced; at around V_{BR}, N x $C_J \approx 60$ pF, or $C_J \approx 90$ fF.

Observing noise

An MPPC generates three noise components: dark noise (or dark counts), afterpulses, and optical crosstalk. Thermally-generated charge carriers that trigger an avalanche are responsible for dark noise. Dark noise is random and is always present regardless of the light level illuminating the MPPC. Its rate (number of pulses per unit time) increases with temperature and ΔV. The presence of the other two noises is correlated to the

occurrence of an avalanche, which has been triggered either by a photo-generated or thermally-generated (dark) charge carrier. A release of a trapped charge in a pixel experiencing an avalanche can trigger a secondary avalanche while the pixel is recovering from the primary avalanche. This is afterpulsing. Optical crosstalk arises when an avalanche in a pixel emits photons that trigger one or more avalanches in the adjoining pixels. The resulting output signal is a superposition of the signals from the "fired" pixels.

Figure 11 illustrates an experimental setup to observe and record the three noise components. An MPPC is inside a temperature-controlled dark box. The variable high voltage source (e.g., Keithley 487) reverse-biases the MPPC and sets the value of ΔV. The output signal from the MPPC is AC coupled to a "fast" amplifier (e.g., Hamamatsu C5594) using a 10 kΩ load resistor and 100 nF coupling capacitor. The output of the amplifier connects to a digital oscilloscope (e.g., LeCroy Wave Pro 7300A). The values of the load resistor and the coupling capacitor can be adjusted to optimize the fidelity of the displayed signals.

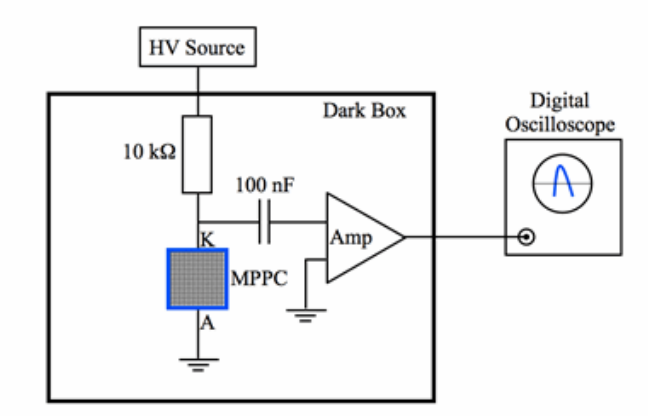

Figure 11. Experimental setup to observe the noise components in an MPPC.

Figure 12 is an example of an oscilloscope display showing an accumulation of waveforms (the persistence was set to 10 s) resulting from the three types of noise. The most numerous waveforms are due to random dark noise. Such a waveform is indistinguishable from the one that would have been produced had the avalanche been triggered by a photo-generated charge carrier. A waveform due to afterpulsing trails (in time) the primary waveform – a waveform due to dark noise. The delay is on the order of tens of ns. The signals due to optical crosstalk are practically in phase with the primary signal and, thus, the resulting waveform is the superposition of the signals. Those that are labeled 2 p.e. (3 p.e.) result when one (two) neighboring pixel is (are) affected.

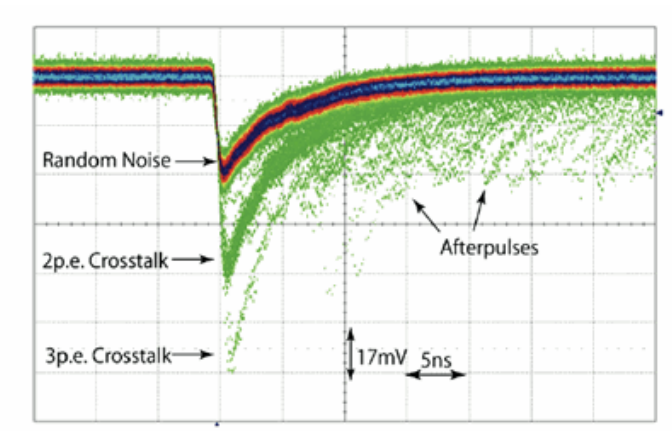

Figure 12. Oscilloscope display (10 s persistence) showing waveforms corresponding to random dark noise,

correlated noise due to afterpulsing, and correlated noise due to optical crosstalk. Adapted from Murase et al. (2009).

Measuring crosstalk

In the absence of light, 2 p.e. (or greater) waveforms originating from an MPPC can be either due to random dark noise occurring in two or more pixels simultaneously or crosstalk. The probability of the former is very small and will be neglected. Therefore, counting the number of waveforms above the 1 p.e. threshold per unit time yields the crosstalk rate, while dividing this rate by the rate of 1 p.e. waveforms yields the crosstalk probability.

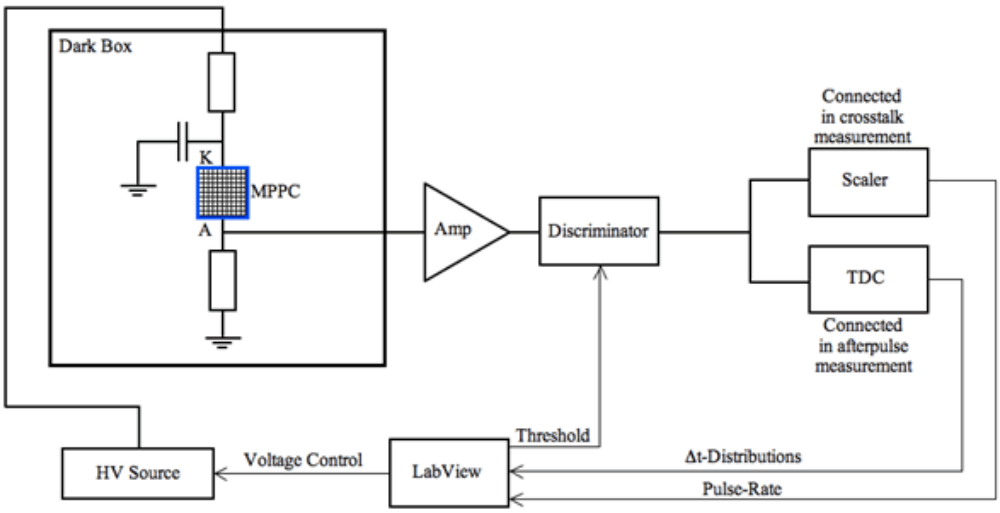

Figure 13. Experimental setup to measure the rates of crosstalk and afterpulsing. Adapted from Eckert et al. (2010).

Figure 13 is an experimental setup to measure the rates (and probabilities) of crosstalk and afterpulsing. The MPPC is inside a temperature-controlled and light-leak-proof dark box reversed-biased by a high voltage source. The amplifier amplifies the output signal from the MPPC and feeds the resulting signal to the discriminator. If the input crosses a user-specified threshold level, the discriminator issues a logical output pulse of some duration (several ns), which the Scaler module, with its gate set to 1 s, counts. Figure 14 shows an example of a resulting count rate as a function of the threshold level for the Hamamatsu S10362-11-050C MPPC operating at ΔV = 1.3 V.

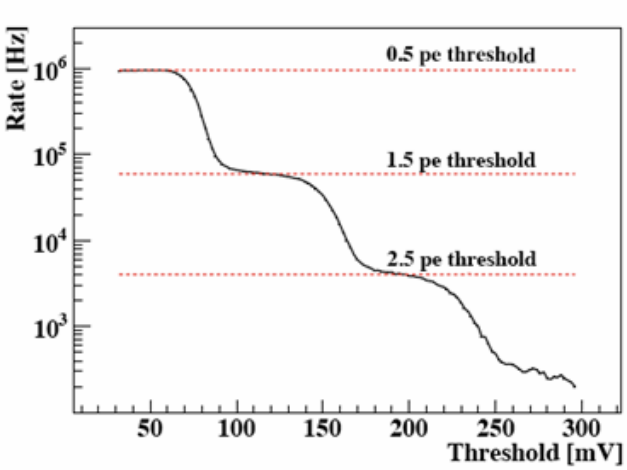

Figure 14. Noise rate as a function of the discriminator threshold for the Hamamatsu S10362-11-050C MPPC operating at ΔV = 1.3 V. Adapted from Eckert et al. (2010).

Figure 14 shows that the noise rate, ν, decreases with the discriminator threshold level showing a characteristic step-like dependence. The horizontal red dashed lines delineate the values of ν for the threshold levels that correspond to 0.5 p.e., 1.5 p.e., and 2.5 p.e., respectively. Setting the threshold level to 0.5 p.e., which is above the electronic noise but below 1 p.e., gives the rate of the total dark noise $\nu_{0.5\ p.e.}$. Setting the threshold to 1.5 p.e. gives the rate of the events due to crosstalk $\nu_{1.5\ p.e.}$. The probability of crosstalk P_C is therefore given by $P_C = \nu_{0.5\ p.e.} / \nu_{1.5\ p.e.}$.

The crosstalk probability P_C depends on the overvoltage ΔV, and the experimental setup depicted in Figure 13 can also be used to determine this dependence. The procedure is to measure P_C as outlined above for different values of ΔV, which is controlled by the high voltage source. Figure 15 is an example of the resulting dependence (note that the gain and ΔV are linearly proportional to each other). The figure shows that P_C steeply increases with ΔV for all of the tested MPPCs.

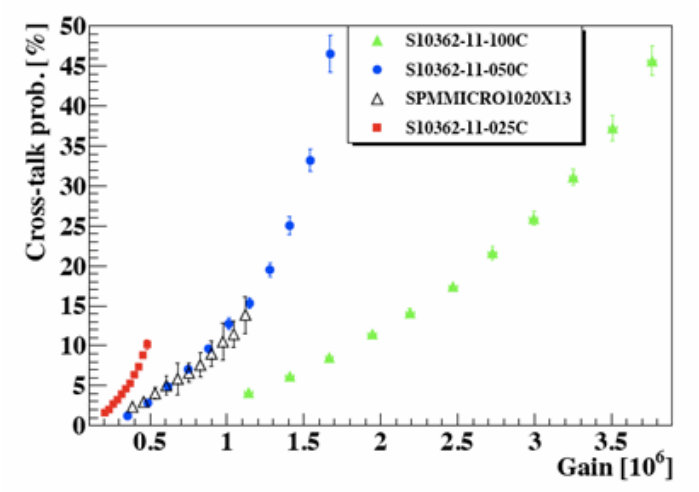

Figure 15. Crosstalk probability as a function of gain (proportional to ΔV). Adapted from Eckert et al. (2010).

Measuring afterpulsing

When a pixel develops an avalanche, some charge carriers can be trapped by lattice defects. Their subsequent release, while the pixel recovers from the primary avalanche, can trigger a secondary correlated avalanche – an afterpulse. The amount of charge released in an afterpulse depends on the time delay δt between the primary and secondary avalanches, or the recovery state of the pixel. The ratio of charge released in an afterpulse and that released in the primary avalanche can be modeled by the following equation.

$$\xi(\Delta t) = 1 - \exp\left(-\frac{\Delta t}{\tau_r}\right)$$

Equation 2. Charge ratio.

In this equation, τ_r is the recovery time (from an avalanche) of a pixel. If δt is small compared to τ_r, then ξ is small implying that an afterpulse has amplitude less than 1 p.e. The amplitude of an afterpulse increases as δt

increases and in the limit $\delta t >> \tau_r$ it is 1 p.e. In this limit, the afterpulse is indistinguishable from a signal that was generated either thermally or optically.

An experimental setup depicted in Figure 13 can be used to measure the probability of afterpulsing P_{ap}. Here, the Scaler is replaced with Time to Digital Converter (TDC), which measures δt for consecutive pulses coming from the discriminator (threshold level at 0.5 p.e.). The solid black curve in Figure 16 is an example of the measured dark noise time-difference distribution. For $\delta t < 20$ ns, the distribution is unreliable because to detect an afterpulse, the primary signal must fall below the discriminator threshold level; the time to do so is on the order of 10 – 15 ns (see Figure 12). For δt greater than the pixel recovery time, the dark-noise time-difference distribution can be modeled as the sum of two probability density functions (what follows is from Eckert et al. 2010).

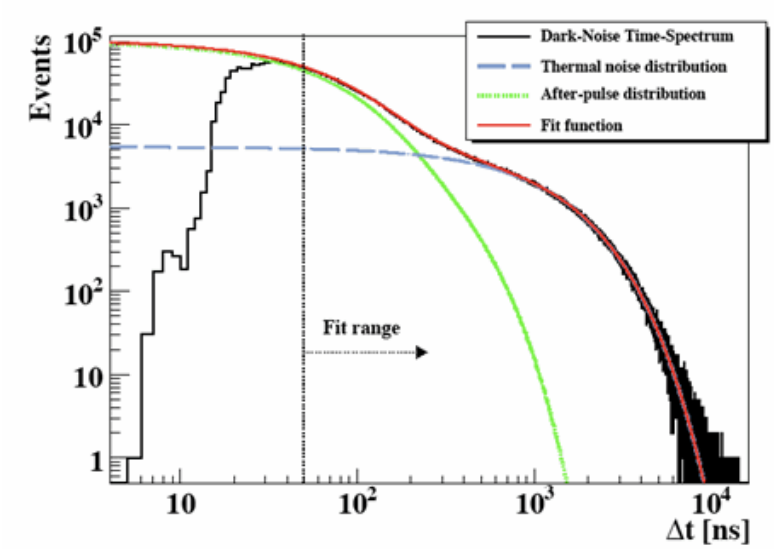

Figure 16. Dark noise time-difference distribution (black solid curve) for Hamamatsu S10362-11-050C at a reverse bias of 70.6 V. Adapted from Eckert et al. (2010).

Equation 3 is a model probability density function for events due to thermal pulses. Here, N_{tp} is the integrated number of thermal events and $1/\tau_{tp}$ is the rate (or frequency) of these events.

$$n_{tp}(\Delta t) = \frac{N_{tp}}{\tau_{tp}} \exp\left(-\frac{\Delta t}{\tau_{tp}}\right)$$

Equation 3. Probability density function for events due to thermal pulses.

Equation 4 is a model probability distribution function for events due to afterpulsing. The function is a sum of two exponentials: the first exponential term models "fast" events with a characteristic time τ_{apf}, whereas the second models "slow" events with a characteristic time τ_{aps}. The parameters N_{apf} and N_{aps} are the integrated number of "fast" and "slow" events, respectively.

$$n_{ap}(\Delta t) = \frac{N_{apf}}{\tau_{apf}} \exp\left(-\frac{\Delta t}{\tau_{apf}}\right) + \frac{N_{aps}}{\tau_{aps}} \exp\left(-\frac{\Delta t}{\tau_{aps}}\right)$$

Equation 4. Probability density function for events due to afterpulses.

The probability density functions given by Equation 3 and Equation 4 are simultaneously fitted to the data, as shown in Figure 16. The fit yields the values of the adjustable parameters in the probability density functions.

With the adjustable parameters determined from the fit, Equation 5 can be used to calculate the probability of afterpulsing. Equation 2 gives the charge ratio function ξ. To evaluate the integral it is necessary to adopt the appropriate pixel recovery time τ_r.

$$P_{ap} = \frac{\int_0^\infty \xi n_{ap} d\Delta t}{\int_0^\infty \xi \left(n_{ap} + n_{tp}\right) d\Delta t}$$

Equation 5. Probability of afterpulses.

The probability of afterpulses P_{ap} is a function of overvoltage ΔV for two reasons. As ΔV increases: (1) the amount of charge in a primary avalanche increases making charge trapping more likely and (2) the probability that a charge carrier triggers an avalanche in the depletion region increases. The same experimental setup and analysis as described above can be used to determine how P_{ap} depends on ΔV by varying the bias voltage on the MPPC. Figure 17 is an example of such dependence for three MPPCs manufactured by Hamamatsu.

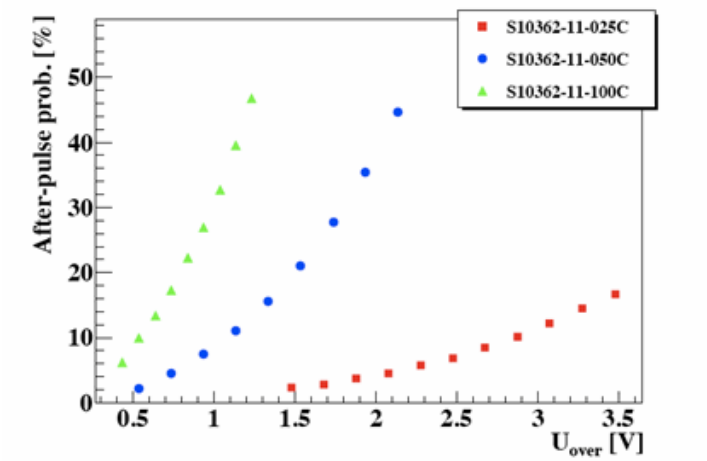

Figure 17. Probability of afterpulsing as a function of overvoltage. Adopted from Eckert et al. (2010).

Measuring photon detection efficiency

The photon detection efficiency, PDE, of an MPPC is defined as the product of quantum efficiency η, the geometrical fill factor F_g, and a combined probability P_a of electrons and holes initiating Geiger-mode avalanche; that is, PDE = $\eta F_g P_a$. The value of η is a probability that a photon generates a charge carrier that enters the avalanche region in a pixel. It is a function of the wavelength of light λ and temperature T, but it is independent of ΔV for full depletion. The geometrical fill factor F_g is a ratio of the combined photosensitive area to the total area of an MPPC. Due to edge effects, F_g exhibits a weak dependence on ΔV. The avalanche probability P_a is a function of λ, T, and ΔV.

The PDE is a crucial parameter in photon counting experiments; therefore, its value must be known for a given

wavelength and overvoltage if absolute photon fluxes are to be measured.

PDE versus overvoltage

Figure 18 shows an experimental setup to measure the PDE of an MPPC as a function of ΔV using a pulsed-LED method discussed in Musienko et al. (2006) and Vacheret et al. (2011).

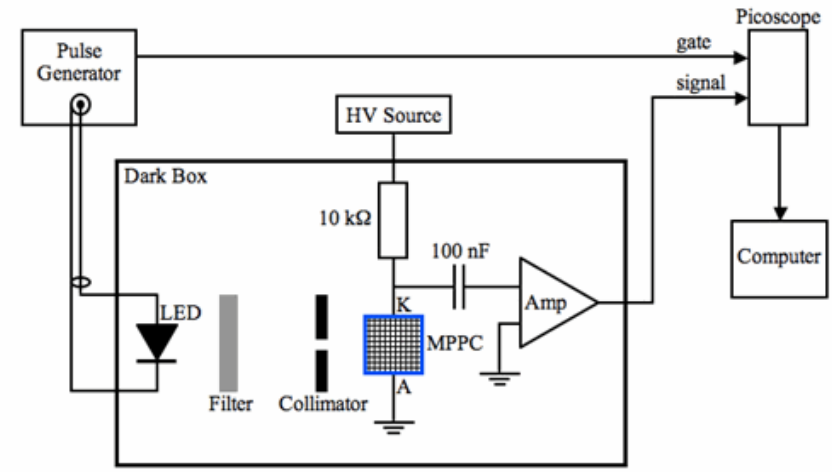

Figure 18. Experimental setup to measure PDE as a function of overvoltage.

An LED with a narrow emission spectrum emits pulses of light with a duration and repetition rate set by the pulse generator. The neutral density filter controls the number of photons per pulse, and the collimator allows a uniform illumination of the photosensitive section of an MPPC. The optical depth of the filter is adjusted so that 2 to 5 pixels are activated per pulse. The number of photons per pulse Nγ arriving at the plane of the MPPC must be measured using a calibrated photodetector, such as the XP2020 or R7899 PMTs. The high-voltage source, such as the Keithley 487, reverse-biases an MPPC and determines the value of ΔV. A fast transimpedance amplifier amplifies the output signal, and the picoscope, such as the PicoScope 5023, digitizes and integrates the output to obtain a charge amplitude spectrum such as the one shown in Figure 19.

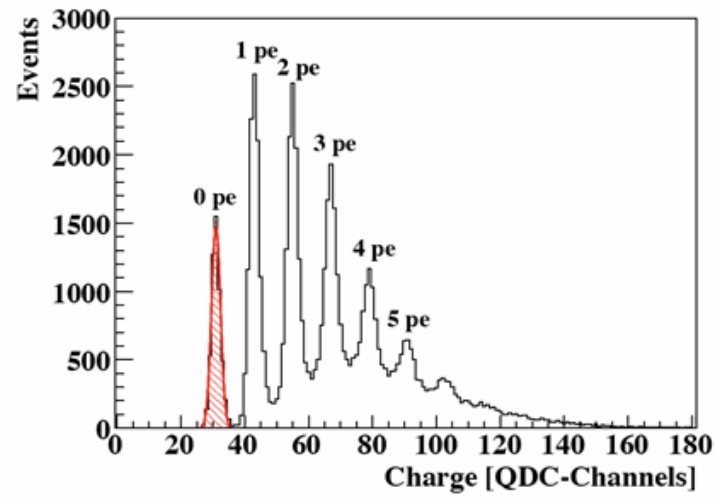

Figure 19. Example of single photon charge spectrum. A peak in the spectrum corresponds to a certain number of photoelectrons, e.g., 0 pe, 1 pe, etc. Adapted from Eckert et al. (2010).

The probability *P* of detecting *n* photons by an MPPC is given by the Poisson distribution.

$$P\left(n, n_{pe}\right) = \frac{n_{pe}^{n} e^{-n_{pe}}}{n!}$$

Equation 6. The probability of detecting *n* photons by an MPPC is given by Poisson distribution.

In this equation, n_{pe} is the average number of photoelectrons. The events for $n = 0$ (no photon detected) correspond to the "pedestal" on the charge amplitude spectrum; the subsequent peaks are for n =1, 2, … (see Figure 19). The values of $P(n, n_{pe})$ for n > 0 are distorted by the presence of crosstalk and afterpulsing, but the value for $n = 0$ is not. Measuring $P(0, n_{np})$, which is the ratio of the number of events in the pedestal N_0 and the total number of events N_T, allows unbiased determination of n_{pe}. Both N_0 and N_T are determined from the charge amplitude spectrum. Since $P(0, n_{pe}) = N_0/N_T = exp(-n_{pe})$, then $n_{pe} = -ln(N_0/N_T)$. Taking into account dark pulses, n_{pe} is given by the following.

$$n_{pe} = -\ln\frac{N_0}{N_T} + \ln\frac{N_0^D}{N_T^D}$$

Equation 7. Average number of photoelectrons.

Here, N_0^D and N_T^D are the number of events in the pedestal and the total number of events, respectively, in a charge amplitude spectrum taken under dark conditions (see Figure 20). Thus, the PDE is given by Equation 8.

$$PDE = \frac{n_{pe}}{N_\gamma}$$

Equation 8. The PDE is a ratio of the average number of photoelectrons and the average number of photons per pulse.

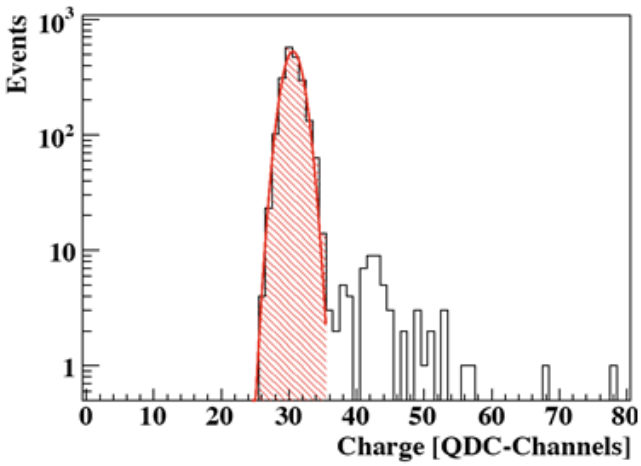

Figure 20. Thermal noise charge spectrum taken under dark conditions. Adopted from Eckert et al. (2010).

Measuring gain and breakdown voltage

A charge amplitude spectrum of an MPPC, such as the one depicted in Figure 19, can be used to determine the gain M of the device using the following equation.

$$M = \frac{QDC_{cal}}{eK_{amp}}\Delta_{pp}$$

Equation 9. Gain of an MPPC using information from charge amplitude spectrum.

In the equation, QDC_{cal} is the charge per one channel of QDC (charge to digital converter), δ_{pp} is the number of channels separating two adjacent peaks, K_{amp} is the amplification factor of the electronics, and e is the value of the fundamental charge. If charge amplitude spectra are collected for various settings of V_{BIAS}, M as a function of V_{BIAS} can be determined, as shown in Figure 21.

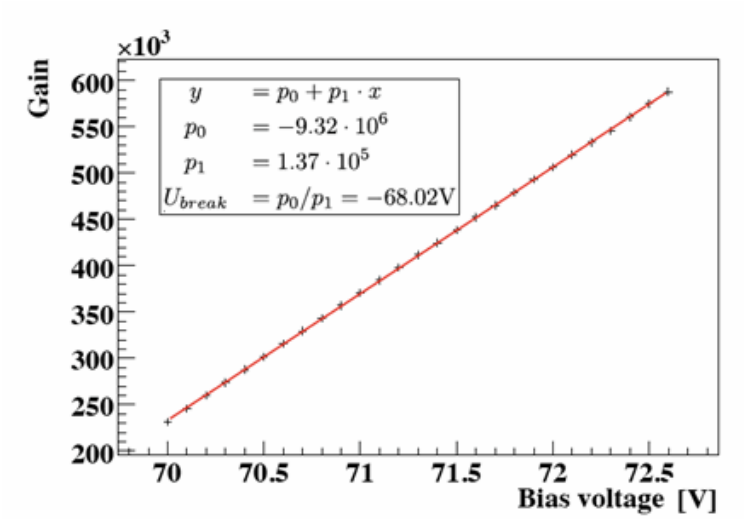

Figure 21. Gain versus bias voltage. Adapted from Eckert et al. (2010).

As expected, the relationship between M and V_{BIAS} is linear with the slope and vertical-intercept equal to C_J/e and C_JV_{BR}/e, respectively. Fitting a straight line to the data yields the values of C_J and V_{BR}.

Measuring time jitter

Suppose that a photodetector is illuminated with δ-function pulses of light that are equally spaced in time with period T and, in response, the detector produces output signal pulses. If the time interval between the consecutive output pulses varies, the output does not have the same period T and the detector is said to exhibit "time jitter."

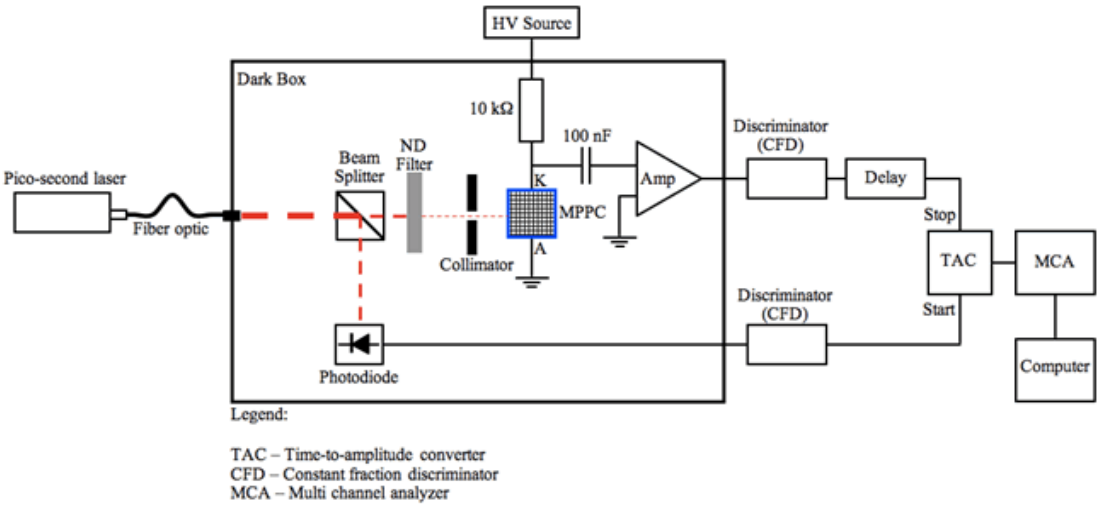

Figure 22. A possible experimental setup to measure the time jitter of an MPPC used by Nagano et al. (2012).

Figure 22 shows a possible experimental setup (Nagano et al. 2012) to measure the time jitter of an MPPC. The detector is inside a temperature-controlled dark box. A pico-second laser (λ = 650 nm, 70 ps pulse width, 1 kHz repetition rate, and time jitter less than 10 ps) is the source of light. The beam splitter divides the beam into two beams. One illuminates a photodiode and the other - after passing through a neutral density filter and collimator - the MPPC. The filter and collimator combination can be adjusted to vary the number of photons per pulse striking the MPPC. The output from the photodiode, after passing through a constant fraction discriminator (CFD), provides the "start" pulse to the time-to-amplitude (TAC) converter. The role of the CFD is to filter out noise: only those signals for which the value of the leading edge exceeds some fraction (e.g., 30%) of the difference between the peak value and the base level are permitted. After being amplified by a factor of 30 to 50, the output from the MPPC passes through the CFD and delay circuit (or line) and arrives at the TAC providing the "stop" pulse. The TAC outputs a signal whose amplitude is proportional to the time difference between the start and stop pulses. The multi-channel analyzer (MCA) stores and sorts the pulses according to their height, and displays their histogram, or spectrum, such as that displayed in Figure 23.

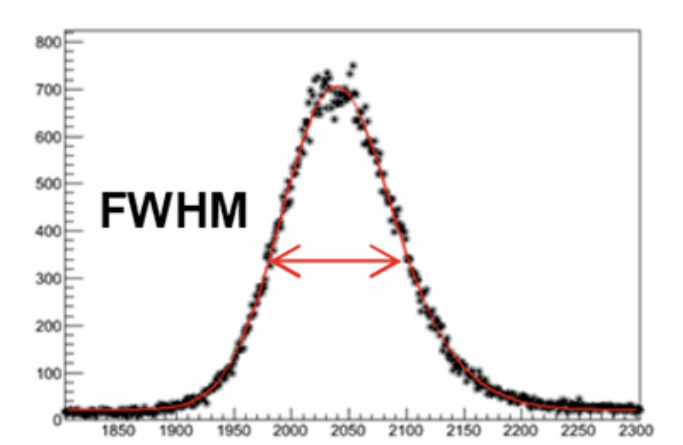

Figure 23. Histogram produced by MCA. The horizontal axis is proportional to the time difference between the "start" and "stop" pulses arriving at the TAC. Adapted from Nagano et al. (2012).

For a normal distribution, the full-width at half maximum (FWHM) is a measure of the total time jitter: FWHM = $2.355\sigma_T$. If the time jitters of the individual components of the setup are independent of one another, the sum of their squares equals σ_T^2. From the time jitters of the laser pulses, photodiode, and the combined

electronics, the time jitter of the MPPC can be calculated.

Measuring linearity and dynamic range

An MPPC consists of N pixels where each pixel can exist in only two states: ON or OFF. A pixel in the OFF state switches to the ON state if it absorbs one or more photons and the resulting photo-generated charge carriers trigger an avalanche. The maximum possible output signal from an MPPC is N p.e. in response to a δ-pulse of light containing N_γ photons. Thus, the total number of pixels determines the dynamic range of the detector.

Equation 10 is a model that gives the number of pixels that have turned ON (or that have "fired") in response to N_γ of incident photons on the surface of an MPPC with N pixels and the photon detection efficiency PDE.

$$N_f = N\left(1 - e^{\frac{-N_\gamma \cdot PDE}{N}}\right)$$

Equation 10. Number of pixels N_f that have turned ON ("fired") in response to N_γ of incident photons on an MPPC with N pixels and the photon detection efficiency PDE.

If the product of N_γ and PDE is much smaller than N, Equation 10 reduces to $N_f = N_\gamma PDE$. Here, the response of the detector is linear with PDE being the constant of proportionality between N_f and N_γ. However, in the limit $N_\gamma PDE \rightarrow \infty$, $N_f \rightarrow N$, the saturation limit.

Gruber at al. (2014) have investigated how a variety of MPPCs respond to pulses of light (32 ps FWHM duration and λ = 404 nm) containing from one to thousands of photons using a setup depicted in Figure 24. The PIN photodiode can be calibrated at low light levels (where $N_\gamma PDE << N$) so that its output is proportional to $N_{seed} \equiv N_\gamma PDE$ at any light level. Here, N_{seed} is the average number of photons incident on the photosensitive area of an MPPC. Thus, the output from the PIN photodiode yields N_{seed} and the scope yields the height of the output signal, which is proportional to N_f. The setup, thus, allows a measurement of N_f as a function of N_{seed} for different settings of overvoltage and of different MPPCs. The results can be normalized to allow a direct comparison among the MPPCs used in the tests and comparison to the predictions from Equation 10.

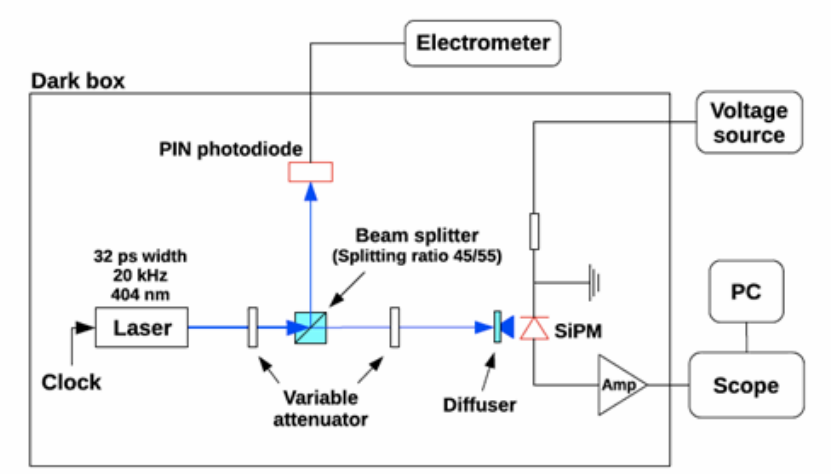

Figure 24. Experimental setup to investigate linearity and saturation limit of MPPCs. Adapted from Gruber et

al. (2014).

The results are surprising. Figure 25 shows the response curves of four different MPPCs normalized to the total number of pixels in each MPPC for high light levels (left panel) and medium to low light levels (right panel). The figure shows that the outputs from the MPPCs are fairly linear and consistent with Equation 10 up to $N_{seed}/N \approx 0.5$. Above this limit, the outputs are larger than the predictions from Equation 10 (Equation 3 in the original study) and the saturation level may be more than 2N (Hamamatsu 050U MPPC), in disagreement with Equation 10. The study finds no acceptable explanation for this "oversaturation" and questions out current understanding of how the device operates.

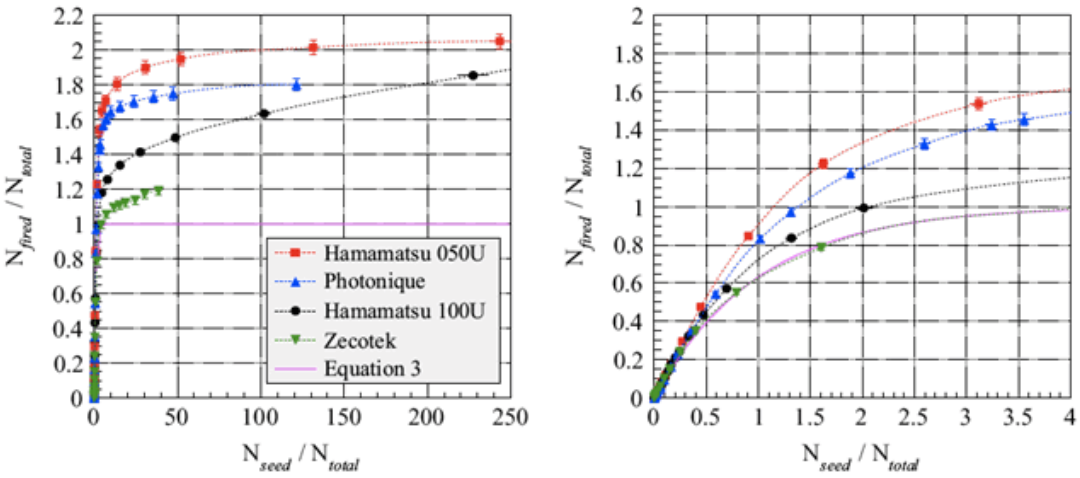

Figure 25. Response curves of four MPPCs for high light levels (left panel) and medium to low light levels (right panel). Adapted from Gruber et al. (2014).

Section III: Summary

This article is a review of the experimental methods to characterize optical and electrical properties of an MPPC. The following are the main points of the article:

1. An MPPC is an array of pixels connected in parallel where one pixel is a series combination of an APD and a quenching resistor. The APD is externally biased to operate in Geiger mode.
2. The junction capacitance and quenching resistance are key electrical parameters of an MPPC. Both can be measured from forward and reverse I-V characteristics of the device.
3. Three major sources of noise exist in an MPPC: thermally-induced random dark counts, correlated optical crosstalk, and afterpulsing. The rates of these noises as a function of temperature and overvoltage can be measured, and these rates will enter into the calculations of the photon flux on the detector.
4. Photon detection efficiency is a ratio of the detected number of photoelectrons to the number of photons in a pulse of light. Knowing how this parameter depends on the wavelength of light and overvoltage is crucial in all photon counting experiments. This article describes a method of measuring this parameter, correcting for the presence of noise.
5. The time interval between the instant when a photon strikes a pixel of an MPPC and the instant the device produces an output varies in a sequence of events. The rms of the variation is known as time jitter - a

crucial characteristic in experiments involving time-of-flight or coincidence. Time jitter is a function of the wavelength of light, overvoltage, and temperature. This article describes a method of measuring this parameter.

6. The total number of pixels of an MPPC limits its dynamic range.
7. The output of an MPPC is linear in a regime where the product of the number of the incident photons and the photo detection efficiency is much smaller than the total number of pixels. MPPCs exhibit a phenomenon of "oversaturation" where the output signal may exceed N p.e. (N is the number of pixels) in response to a pulse of light containing N_γ of photons. This phenomenon is not well understood.

References

P. Eckert, H.C. Schultz-Coulon, W. Shen, R. Stamen and A. Tadday, "Characterization studies of silicon photomultipliers," *Nucl. Instrum. and Meth.* A 620 (2010): 217-26.

R. H. Haitz, "Model for the Electrical Behavior of a Microplasma," *J. of Appl. Phys.,* vol. 35, no. 2 (1964): 1370-1376.

L. Gruber, S. E. Brunner, J. Marton, K. Suzuki, "Over saturation behavior of SiPMs at high exposure," *Nucl. Instrum. Meth.* A 737 (2014): 11-18.

R. J. McIntyre, "Theory of Microplasma Instability in Silicon" *J. of Appl. Phys.,* vol. 32, no. 6 (1961): 983-995.

T. Murase, H. Oide, H. Otono, S. Yamashita, "Development of PPD: characterization and simulation," International Workshop on New Photon Detectors PD09, June 24-26 2009, Shinshu University, Matsumoto, Japan.

Y. Musienko, S. Reucroft and J. Swain, "The gain, photon detection efficiency and excess noise factor of multi-pixel Geiger-mode avalanche photodiodes," *Nucl. Instrum. Meth.* A 567 (2006): 57.

T. Nagano, K. Sato, A. Ishida, T. Baba, R. Tsuchiya, K. Yamamoto, "Timing Resolution Improvement of MPPC for TOF-PET Imaging," 2012 IEEE Nuclear Science Symposium and Medical Imaging Conference Record (NSS/MIC).

A. Vacheret , G. J. Barker , M. Dziewiecki , P. Guzowski , M. D. Haigh , B. Hartfiel , A. Izmaylov , W. Johnston , M. Khabibullin , A. Khotjantsev , Y. Kudenko , R. Kurjata , T. Kutter , T. Lindner , P. Masliah , J. Marzec , O. Mineev , Y. Musienko , S. Oser , F. Retiere , R. O. Salih , A. Shaikhiev , L. F. Thompson , M. A. Ward , R. J. Wilson, N. Yershov , K. Zaremba and M. Ziembicki, "Characterization and simulation of the response of multi-pixel photon counters to low light levels," *Nucl. Instrum. Methods Phys. Res.* A vol. 656, no. 1 (2011): 69-83.